5

The Impact of VBR MPEG Video Traffic on ATM Multiplexer Performance and its Evaluation

Jürgen Enssle
Institute of Commun. Switching and Data Technics *
University of Stuttgart, Seidenstraße 36,
70174 Stuttgart, Germany.
Telephone: +49 711 1212475. Fax: +49 711 1212477.
email: enssle@ind.uni-stuttgart.de

Abstract

The Broadband Integrated Services Digital Network (B-ISDN) will be based on the Asynchronous Transfer Mode (ATM) that allows statistical multiplexing of variable bit rate (VBR) sources to make efficient use of the network resources. The ability of the network elements to apply statistical multiplexing while providing a guaranteed quality of service (QoS) to the users is depending on the statistical properties of the ATM traffic streams. Thus it is essential to investigate the multiplexing behaviour of different ATM traffic streams with respect to the ATM QoS parameters cell loss, cell delay and cell delay variation using realistic source models. Since compressed video data will have a major share in future broadband traffic and the MPEG coding algorithm up to now has achieved wide popularity, we will concentrate on VBR MPEG video data streams. The flexible hierarchical source model presented in [Enss 95], that is capable of modelling VBR MPEG video and other sources that exhibit long range dependence (LRD) and/or periodic properties, is used to investigate in detail the multiplexing behaviour of such sources.
The focus of this paper is twofold. First, the consequences of the usage of LRD traffic streams in discrete event simulations in terms of the necessary simulation duration and the convergence to a steady state behaviour are investigated. Therefore, we will investigate how the convergence rate of the

*The author is meanwhile with the Alcatel Telecom Research Division, Stuttgart, and may be reached via jenssle@rcs.sel.de

©IFIP 1997. Published by Chapman & Hall

confidence interval size of the empirical mean value of discrete stochastic processes depends on the Hurst parameter.
Second, it will be shown that both, the LRD and periodic traffic components have a significant impact on the multiplexer performance in terms of the cell loss probability and the cell delay but mainly act on different time scales. The actually noticeable influence on the quality of service (QoS), that the VBR MPEG video data streams perceive, depends on the multiplexer buffer size and the stochastic properties of the video data streams at the different time scales.

1 INTRODUCTION

The Broadband Integrated Services Digital Network (B-ISDN) will be based on the Asynchronous Transfer Mode (ATM) that uses packets with a constant length of 53 bytes called cells. It allows statistical multiplexing of variable bit rate (VBR) sources to make efficient use of the network resources. The ability of the network elements to apply statistical multiplexing while providing a guaranteed quality of service (QoS) to the users is, besides the total load offered, decisively depending on the statistical properties of the ATM traffic streams. Thus it is essential to investigate the multiplexing behaviour of different ATM traffic streams with respect to the ATM QoS parameters cell loss, cell delay and cell delay variation using realistic source models.

Video data will have a major share in future broadband traffic due to the introduction of video on demand services, conferencing services and as a main constituent of multimedia applications. Since the beginning of the MPEG (Motion Pictures Experts Group) standardization efforts [MPEG 1, MPEG 2], the MPEG coding technique has achieved wide popularity. Therefore, we will investigate the multiplexing behaviour of MPEG encoded video data streams. Due to the different structure and complexity of the consecutive pictures of a video, the compression of the video data inherently results in a VBR video data stream if a constant picture quality shall be attained. To investigate the impact of VBR MPEG encoded video data streams on the network elements, stochastic models are used to characterize the behaviour of the video sources and the associated ATM traffic streams.

Generally, the behaviour of a video source and thus the stochastic characteristics of the associated ATM VBR video data stream depend on the coding technique, the application and the video contents itself. These influences act on different time scales. At least three levels can be distinguished, namely the cell level, the picture level and the scene level. The behaviour at the cell level is dominated by the ATM packetization process. The encoder algorithms and parameters essentially determine the picture level. Finally, the scene level is mainly governed by the fluctuations in the amount of information in consecutive pictures. The amount of information depends on the contents and type of the video material and is independent of the coding algorithm.

Recent research results indicate that VBR video traffic exhibits a property called long range dependence (LRD) or persistence [Cox 84, Hurs 51] that can be characterized by the Hurst parameter H [Enss 95, GaWi 94, GFA 96]. Long range dependent traffic streams are highly correlated and in the case of video data even pictures a long time span apart cannot be considered independent of each other. The LRD property mainly results from the different complexity of consecutive pictures. Therefore, the Hurst parameter H is depending on the movie contents and varies over a broad range of values [Rose 95], but it is almost independent of the video coding algorithm. The offered traffic volume per picture is characterized by highly asymmetrical empirical probability distribution functions (PDFs) that can be approximated by lognormal PDFs [HTL 94, KSH 95]. VBR MPEG video data streams additionally reveal periodic components due to the application of three different picture types with different compression ratios. The fact that VBR MPEG video data streams exhibit LRD and periodic properties has a significant impact on the ATM multiplexer performance, but also affects its evaluation using discrete event simulations. Thus, the focus of this paper is twofold to quantify these influences.

The ATM multiplexer performance results that will be presented in this paper are based on discrete event simulations conducted using the hierarchical VBR MPEG source model presented in [Enss 95]. It uses three lognormal distribution functions to model the size of the I-, P- and B-pictures at the picture level. These distribution functions are derived from a fast fractional Gaussian noise (ffGn) random process via a transformation that takes the MPEG GOP (group of pictures) pattern into account. The ffGn random process models the long range dependent fluctuations of the picture information contents at the scene level. It is an approximation of the fractional Gaussian noise process suited very well for computer simulations.

The remaining of the paper is organized as follows: First, we will briefly describe the main characteristics of the MPEG encoding algorithm that are reflected in the source model and restate the VBR MPEG source model as far as necessary for the following sections. Then, the impact of the use of LRD VBR traffic streams on the convergence of discrete event simulation results is investigated. Next, the performance of an ATM multiplexer, that is fed by a number of VBR MPEG video data streams, is evaluated. The main results will be presented and conclusions will be given.

2 VBR MPEG VIDEO ENCODING

The MPEG video coding standard uses a combination of intra- and interframe coding because of the conflicting requirements of random access and highly efficient compression. The use of motion compensation allows to exploit temporal redundancy in the video sequence. Spatial and perceptual redundancy

reduction is achieved via Discrete Cosine Transform (DCT) coding and quantization of the DCT coefficients.

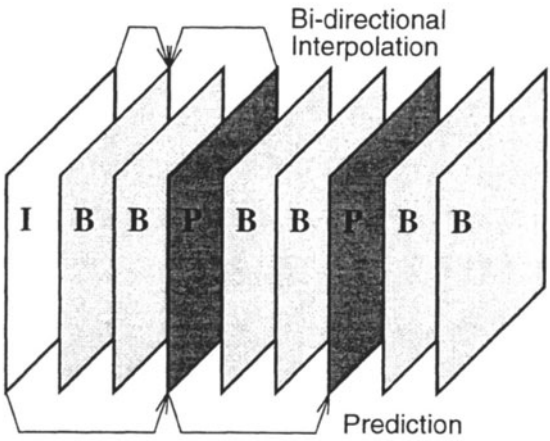

Figure 1 MPEG GOP pattern ($N = 9$, $M = 3$)

Three main picture types are defined. Intra coded pictures (I-pictures) are coded without reference to other pictures. Predictive coded pictures (P-pictures) are coded more efficiently using motion compensated prediction from a past I- or P-picture. Bidirectionally-predictive coded pictures (B-pictures) provide the highest degree of compression using past and future I- or P-pictures as a reference for motion compensation. The three picture types are periodically organized in a so called group of pictures (GOP) defined by the distance N between I-pictures and the distance M between P-pictures. The basic parameters of the model that will be used throughout this paper are derived from the statistics of a sequence (82 minutes) of the movie "Star Wars", that was encoded using an MPEG 1 software encoder. The GOP pattern used for the statistics trace was IBBPBBPBB with $N = 9$ and $M = 3$ (Figure 1). The picture size was set to 640 × 480 pixel at a picture rate of 25 Hz. The sequence length of the statistics trace containing the number of bits necessary to encode the consecutive pictures encompasses 123574 pictures. Its basic statistical properties, that were used for the investigations presented in this paper are listed in Table 1. As can be seen, the use of different coding algorithms results in different compression ratios for the three picture types and the use of three lognormal PDFs is appropriate [Enss 94].

Table 1 Picture size statistics of the Star Wars sample trace

Picture type	Minimum [*bit*]	Maximum [*bit*]	Mean [*bit*]	COV
I	44520	387656	$1.82 \cdot 10^5$	0.24
P	14352	394920	$1.03 \cdot 10^5$	0.33
B	2720	144048	$4.41 \cdot 10^4$	0.32
All	2720	394920	$7.25 \cdot 10^4$	0.72

3 MODELLING

3.1 VBR MPEG Video Source

The picture sizes of the VBR MPEG video data streams are modelled by the hierarchical source model presented in [Enss 95] (see Figure 2) that is based on the GOP-periodic exponential transformation of the fast fractional Gaussian noise random process (ffGN) [Mand 71]. This model takes the first and second order statistical properties and the short and long term correlation characteristics of the VBR MPEG video data streams into account, including long range dependence (LRD) effects. The model can be adapted to represent any MPEG encoded video sequence by seven parameters, that can be derived e. g. from an empirical sequence. In the following, the basic equations necessary to implement the ffGn process for the scene activity generation and the transformantion to get the picture sizes will be presented. The ATM packetization process used for the simulations will be described shortly.

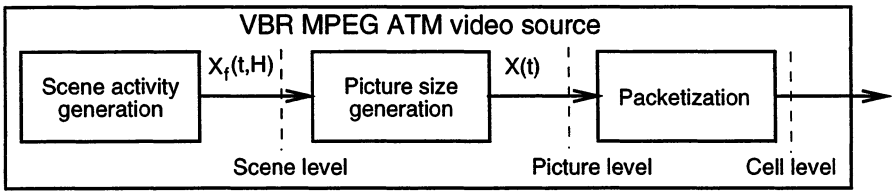

Figure 2 VBR MPEG ATM video source model

At the scene level, an ffGn process is used to approximate the LRD behaviour of video sources at that time scale. The ffGn process $X_f(t, H)$, $t \in I\!N$, $H \in [0.5, 1[$ generates a sequence of N(0,1)-distributed random variables with an autocorrelation function that approximates the autocorrelation function

$$r_{\Delta B_H \Delta B_H}(\tau) = \begin{cases} 1 & \text{for } \tau = 0 \\ \frac{1}{2}\left[(\tau+1)^{2H} - 2\tau^{2H} + (\tau-1)^{2H}\right] & \text{for } \tau > 0 \end{cases} \quad (1)$$

of the discrete fractional Gaussian noise random process ΔB_H, that is exactly second order self-similar. The ffGn process is constructed as the sum of a low frequency term

$$X_l(t,H) = \sum_{k=1}^{N(n_{\mathrm{ffGn}})} W_k \, X_{\mathrm{MG}}(t,r_k) \tag{2}$$

and a high frequency term $X_h(t,H)$. The Markov Gauss processes $X_{MG}(t,r_k)$ are defined as

$$X_{\mathrm{MG}}(t,r_k) = \begin{cases} G_k(1) & \text{for } t=1 \\ r_k \, X_{\mathrm{MG}}(t-1,r_k) + \sqrt{1-r_k^2}\, G_k(t) & \text{for } t>1 \end{cases}, \tag{3}$$

where $G_k(t)$, $k = 1,\ldots,N(n_{\mathrm{ffGn}})$, $t \in \mathbb{N}$ denote sequences of independent standard normally distributed random variables. The lag-1 covariance r_k is defined as

$$r_k = e^{-B^{-k}} \tag{4}$$

and the weight factors W_k are determined by

$$W_k^2 = \frac{H(2H-1)\left(B^{1-H} - B^{H-1}\right)}{\Gamma(3-2H)} B^{-2k(1-H)} \, . \tag{5}$$

The number $N(n_{\mathrm{ffGn}})$ of Markov-Gauss processes depends on the number n_{ffGn} of consecutive random numbers that shall exhibit the LRD property. It is defined by

$$N(n_{\mathrm{ffGn}}) = \lceil \ln(Q \cdot n_{\mathrm{ffGn}}) / \ln(B) \rceil \, . \tag{6}$$

The ffGn process is, besides the time t and the Hurst parameter H, depending on two additional parameters, the base B and the quality Q. These parameters define the accuracy of the approximation of the dfGn random process and its autocorrelation function that is achieved by the ffGn random process. As $B \to 1$ and $Q \to \infty$ the approximation will improve. Reasonable ranges for the parameters B and Q are $B \in [1.1\,,2.0]$ and $Q \in [10\,,20]$ to achieve accurate LRD behaviour [Schu 95]. The high frequency term $X_h(t,H)$ is necessary to correct the variance of the low frequency term so that the random variables of the ffGn random process are N(0,1)-distributed. It has to be chosen according to

$$X_h(t,H) = \sqrt{1 - \frac{H(2H-1)B^{H-1}}{\Gamma(3-2H)}}\, G(t) \tag{7}$$

Table 2 LRD accuracy of the ffGn random process ($B = 2$, $Q = 10$, $n_{\text{ffGN}} = 300000$)

Desired H	0.6	0.7	0.8	0.95
Measured H_{RS}	0.58	0.68	0.79	0.91

where again $G(t)$ is a sequence of independent standard normally distributed random variables. Table 2 shows the resulting Hurst parameter H_{RS} that is measured using the RS-analysis [MaWa 69a, MaWa 69b] in comparison with the desired H that was used as an input parameter for the ffGn process.

Based on the ffGn process $X_f(t, H)$, the picture sizes $X(t)$ are generated using the transformation

$$X(t) = \exp\left[\sqrt{\ln\left(1 + \frac{\text{Var}[X_k]}{\text{E}[X_k]^2}\right)}\, X_f(t, H) + \ln \text{E}[X_k] - \frac{1}{2}\ln\left(1 + \frac{\text{Var}[X_k]}{\text{E}[X_k]^2}\right)\right]. \quad (8)$$

The random variables X_k, $k \in \{I, P, B\}$ denote the I, P and B picture sizes. For the picture size of the picture with number t, $t \in \mathbb{N}$ the parameter k is chosen according to the MPEG GOP pattern. The probability density function $f_X(x)$ of the picture sizes $X(t)$ is given by

$$f_X(x) = \sum_{k \in \{I,P,B\}} p_k f_{X_k}(x)\,, \quad (9)$$

where $f_{X_k}(x)$, $k \in \{I, P, B\}$ denote the lognormal probability density functions of the three picture types and p_k is the probability of finding a picture of type k within the GOP pattern.

The pictures are packetized separately into ATM cells, that are assumed to have a payload of 47 byte. All the cells of a picture have to be transmitted within 40 ms, to achieve a picture rate of 25 Hz. They may be transmitted in a burst at a specified burst bit rate $R_{z,on}$ (the burst bit rate is increased for a single picture if it is too large for the specified rate) or equally spaced over the available 40 ms (in the following this is the default case if no burst bit rate is specified).

3.2 Multiplexer

In order to investigate the feasibility and efficiency of the transmission of VBR video traffic in future ATM systems, understanding the behavior of a

multiplexer and its performance is essential. The ATM statistical multiplexer is modelled as a queue with deterministic service time D corresponding to a link bit rate of R_L Mbit/s and a maximum queue size of S cells. It is fed by N_{Mux} VBR MPEG ATM video sources (Figure 3).

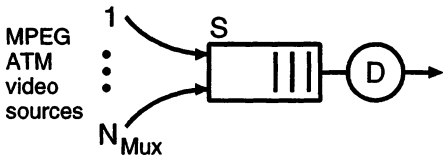

Figure 3 ATM multiplexer model

4 CONVERGENCE OF SIMULATION RESULTS

For the stationary evaluation of a technical system via discrete event simulation, it is essential to assess the convergence of the system behaviour to a steady state. The convergence rate is depending on the system architecture and the correlation structure of the stochastic processes used to model randomly performing system components. In the case of an ATM multiplexer with deterministic service time, the convergence rate is decisively determined by the random processes used to model the sources.

The level of convergence can be described by confidence intervals, that give the interval in that the real value of a variable is located with probability γ (e. g. 95% or 99%), based on the measurements taken during the simulation runs. For a discrete time stochastic process (sequence of random variables) $\{X_t\}$, $t \in \mathbb{N}$, the convergence of its mean

$$X_t^{**} = \frac{1}{t} \sum_{i=1}^{t} X_i \tag{10}$$

is of basic interest. Thus, in the following the convergence of the mean X_t^{**} of a sequence of standard normally distributed random variables $\{X_t\}$ with zero mean and unit variance with different correlation structures will be evaluated in terms of its confidence interval size, since this type of process is used to model the scene level within the VBR MPEG video source model. The confidence interval

$$\left[-z_{\frac{1+\gamma}{2}}, z_{\frac{1+\gamma}{2}}\right] \tag{11}$$

is delimited by the $\frac{1+\gamma}{2}$-quantile $z_{\frac{1+\gamma}{2}}$ with

$$z_{\frac{1+\gamma}{2}} = \Phi^{-1}\left(\frac{1+\gamma}{2}\right) \tag{12}$$

where $\Phi(x)$ denotes the distribution function of the standard normal distribution.

If $\{X_t\}$ is a sequence of independent identically N(0,1)-distributed random variables, X_t^{**} is distributed according to N(0,1/t) and the confidence interval is given by

$$\left[-\frac{1}{\sqrt{t}} z_{\frac{1+\gamma}{2}} \;,\; \frac{1}{\sqrt{t}} z_{\frac{1+\gamma}{2}}\right] . \tag{13}$$

For an exactly second order self-similar standard normally distributed random process, the variance of its mean X_t^{**} is given by [Cox 84] as $\mathrm{VAR}[X_t^{**}] = t^{-2(1-H)}$ and so its resulting confidence interval is

$$\left[-\frac{1}{t^{1-H}} z_{\frac{1+\gamma}{2}} \;,\; \frac{1}{t^{1-H}} z_{\frac{1+\gamma}{2}}\right] . \tag{14}$$

The mean $X_f^{**}(t,H)$ of a standard normally distributed ffGn-process is calculated according to

$$X_f^{**}(t,H) = \sum_{k=1}^{n_{\mathrm{ffGn}}} W_k \frac{1}{t} \sum_{i=1}^{t} X_{\mathrm{MG}}(i, r_k) \;+\; \frac{1}{t} \sum_{i=1}^{t} X_h(i,H) . \tag{15}$$

The random variables of the Markov Gauss process $X_{MG}(t, r_k)$ (see equation 3) can be restated as a moving average process

$$X_{\mathrm{MG}}(t, r_k) = \begin{cases} G_k(1) & \text{for } t = 1 \\ r_k^{t-1} G_k(1) + \sqrt{1 - r_k^2} \sum_{i=2}^{t} r^{t-i} G_k(i) & \text{for } t > 1 \end{cases} . \tag{16}$$

Therefore, their sum can be written as

$$\sum_{i=1}^{t} X_{\mathrm{MG}}(i, r_k) = \sum_{i=1}^{t} r_k^{i-1} G_k(1) + \sqrt{1 - r_k^2} \sum_{j=1}^{t-1} \sum_{i=1}^{t-j} r_k^{i-1} G_k(j+1) . \tag{17}$$

Since the random variables $G_k(t)$ are mutually independent and N(0,1)-distri-

buted, the random variable $\frac{1}{t}\sum_{i=1}^{t} X_{\mathrm{MG}}(i, r_k)$ is $\mathrm{N}(0,\sigma^2_{\mathrm{MG}}(t, r_k))$-distributed with

$$\sigma^2_{\mathrm{MG}}(t, r_k) = \frac{1}{t} + 2\sum_{i=1}^{t-1} \frac{t-i}{t^2} r_k^i \,. \tag{18}$$

Consequently, the weighed sum of all Markov Gauss processes is normally distributed with zero mean and variance $\sigma^2_{\mathrm{MG}}(t)$ with

$$\sigma^2_{\mathrm{MG}}(t) = \sum_{k=1}^{n_{\mathrm{ffGn}}} W_k^2 \, \sigma^2_{\mathrm{MG}}(t, r_k) \,. \tag{19}$$

The high frequency term $X_h(t, H)$ is a sequence of independent identically standard normally distributed random variables with zero mean and variance

$$\sigma_h^2 = 1 - \frac{H(2H-1)B^{H-1}}{\Gamma(3-2H)} \,, \tag{20}$$

hence $\frac{1}{t}\sum_{i=1}^{t} X_h(i, H)$ is $\mathrm{N}(0,\sigma_h^2/t)$-distributed. Finally, $X_f^{**}(t, H)$ is normally distributed with

$$\mathrm{E}[X_f^{**}(t, H)] = 0 \qquad \text{and} \tag{21}$$

$$\mathrm{VAR}[X_f^{**}(t, H)] = \sigma^2_{\mathrm{MG}}(t) + \frac{\sigma_h^2}{t} \tag{22}$$

and its confidence interval to the confidence level γ results in

$$\left[-\sqrt{\sigma^2_{\mathrm{MG}}(t) + \frac{\sigma_h^2}{t}}\, z_{\frac{1+\gamma}{2}} \,,\; \sqrt{\sigma^2_{\mathrm{MG}}(t) + \frac{\sigma_h^2}{t}}\, z_{\frac{1+\gamma}{2}} \right] \,. \tag{23}$$

In Figure 4, the 95% confidence interval sizes for standard normally distributed exactly second order self-similar stochastic processes with different Hurst parameters H are depicted according to equation 14. With increasing H the confidence interval size decreases much slower compared with a sequence of uncorrelated random variables ($H = 0.5$). Consequently, to achieve a desired confidence interval size for the simulation results, the simulation program has to run considerably longer. E. g. to achieve a confidence interval size of 10^{-1} the simulation takes more than four orders of magnitude longer for $H = 0.8$ compared to $H = 0.5$. For $H \to 1$ the confidence interval size even stays constant, independent of the simulation duration. This is an indication for the fact, that the boundary of the stationarity region of the random process is reached.

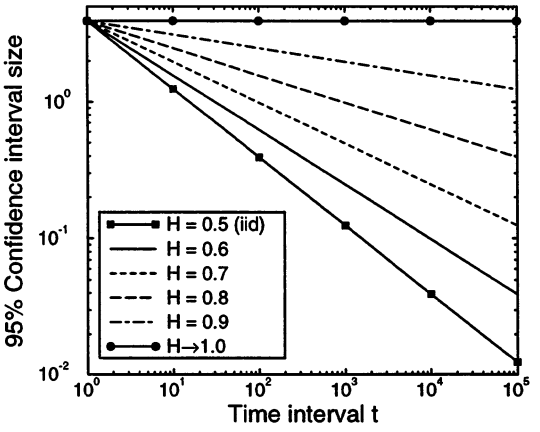

Figure 4 Confidence interval size of X_t^{**} of second order self-similar stochastic processes for varying H

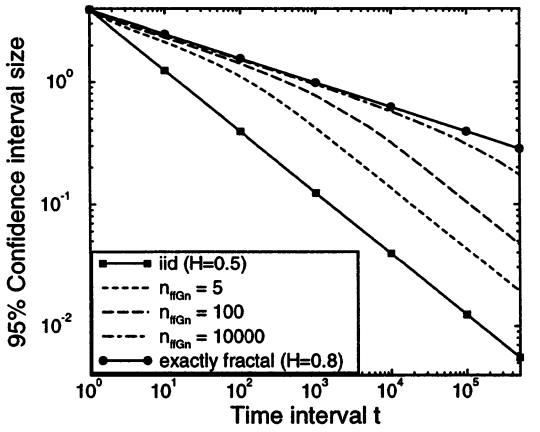

Figure 5 Confidence interval size of the ffGn mean value process $X_f^{**}(t, H)$ ($H = 0.8$, $B = 1.1$, $Q = 20$)

Since the ffGn random process is approximately self-similar, the degree of self-similarity and thus the convergence rate of its mean random process depends on the choice of its parameters B, Q and n_{ffGn}. Figure 5 shows the confidence interval sizes for an ffGn process with $H = 0.8$ in comparison with those of an exactly second order self-similar stochastic process and a sequence of uncorrelated N(0,1)-distributed random variables. The larger the number of desired samples n_{ffGn} is chosen, the better is the ability of the

ffGn process to model the self-similar behaviour. Therefore, for larger values of n_{ffGn} the confidence interval size follows longer the slope of the exactly self-similar random process before it starts to decay as fast as the confidence interval size of the uncorrelated random variables.

5 ATM MULTIPLEXER PERFORMANCE EVALUATION

The performance of an ATM statistical multiplexer is evaluated at the cell, picture and scene level to demonstrate the impact of the source parameters at the different time scales on the multiplexer behaviour and the QoS perceived by the video data streams.

5.1 Cell Level

At the cell level, the way in that the ATM cells of the consecutive pictures are sent determines the short term characteristics of the cell stream. Thus, the packetization process has a strong impact on the performance of a multiplexer with a small buffer. Figure 6 illustrates the influence of the burst bit rate $R_{z,on}$ on the cell loss probability V_z of a multiplexer with a buffer capacity of 50 ATM cells. It clearly shows the increase in the cell loss rate due to the increase of the on-off characteristic of the source cell streams when most of the frames are sent with a burst bit rate larger than the bit rate necessary for an equally spaced play-out.

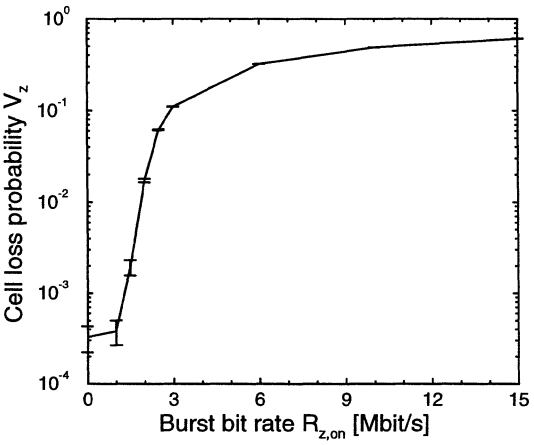

Figure 6 Cell loss probability V_z depending on burst bit rate $R_{z,on}$ ($A = 0.82$, $S = 50$, $N_{\mathrm{Mux}} = 40$, $R_L = 100$ Mbit/s)

5.2 Picture Level

Since the MPEG encoding algorithm uses three different picture types in a periodic GOP pattern, the resulting ATM cell stream reflects the periodic bit rate variations. Therefore, the phase relations of the VBR MPEG ATM cell streams with each other influence the characteristics of the overall input cell stream to the multiplexer and thus its performance. The worst case is that all sources are in phase (identical phase relation), i.e. the start of the GOP patterns of all sources are aligned. The smoothest aggregated cell stream results from a cyclic starting pattern for the GOPs of the different sources (cyclic phase relation).

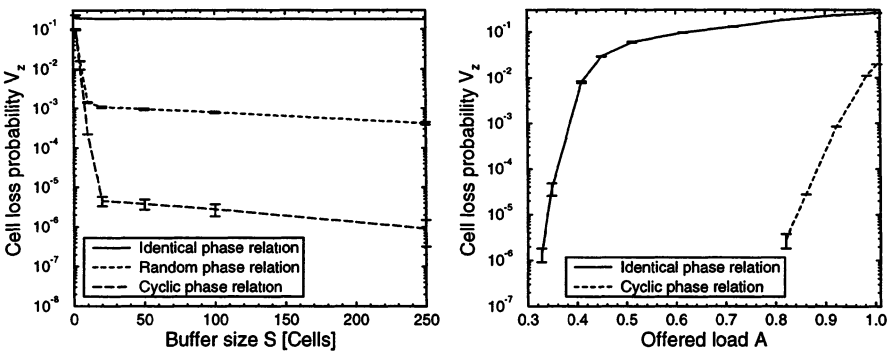

(a) Offered load $A = 0.82$ (b) Buffer size $S = 100$ cells

Figure 7 Cell loss probability V_z depending on the phase relation of the VBR MPEG video data streams ($R_L = 100$ Mbit/s, $H = 0.5$)

Figure 7 (a) shows the dependence of the cell loss probability V_z on the buffer size S for different phase relations. If it is possible to choose a cyclic phase relation, e. g. by a video on demand system, it is possible to lower the cell loss ratio at the picture level by more than four decades. Even compared with the case of a random phase selection the cyclic phase relation achieves a gain of two decades. To achieve a certain cell loss probability the cyclic phase relation increases the admissible load of the multiplexer by a factor of about 2.4 compared with the worst case relation (Figure 7 (b)). The Hurst parameter H has no effect on the cell loss ratio for buffer sizes up to several hundred cells (compare Figure 9). Figure 8 further emphasizes that the Hurst parameter H does not influence the multiplexer behaviour when moderate buffer sizes are used. The probability density functions $f_{S_A}(s)$ of the number of cells S_A that are already waiting in the buffer when a new cell arrives have a pot-like shape and are almost indistinguishable for a Hurst parameter $H \in [0.5, 1.0[$. Therefore, the mean cell delay and the cell delay variation as

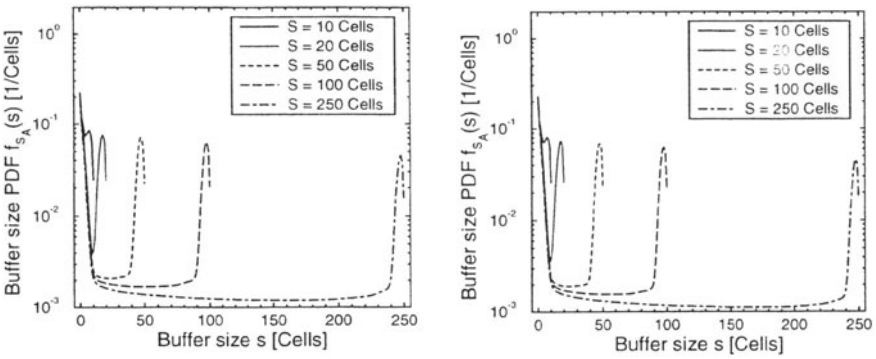

Figure 8 Buffer size probability density function (PDF) $f_{S_A}(s)$ at cell arrivals ($A = 0.93$)

well as the cell loss ratio are independent of the Hurst parameter for medium buffer sizes.

5.3 Scene Level

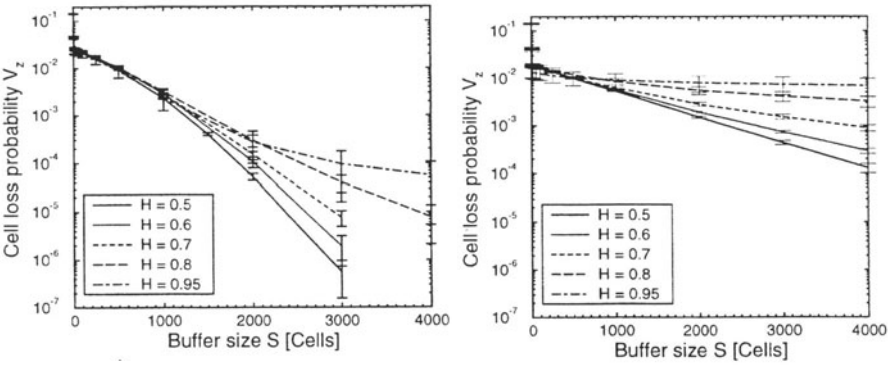

Figure 9 Cell loss probability V_z depending on the multiplexer buffer size S and the Hurst parameter H ($A = 0.93$, $N_{\mathrm{Mux}} = 40$)

The behaviour of VBR MPEG video data streams at the scene level is characterized by the Hurst parameter H, that is mainly depending on the video contents. Figure 9 displays the influence of video data streams with identical probability distribution functions for the picture sizes but different Hurst parameters H on the cell loss probability V_z. For Figure 9 (a) three different

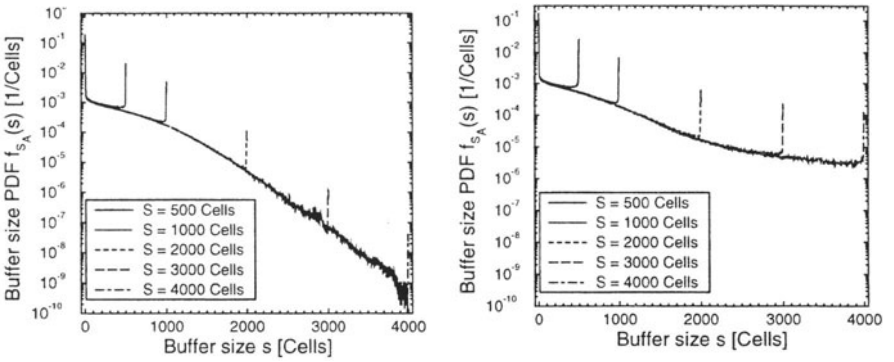

(a) $H = 0.5$ (b) $H = 0.95$

Figure 10 Multiplexer buffer size PDF $f_{S_A}(s)$ depending on the maximum multiplexer buffer size S for the picture types I, P and B ($A = 0.93$, $N_{\mathbf{Mux}} = 40$)

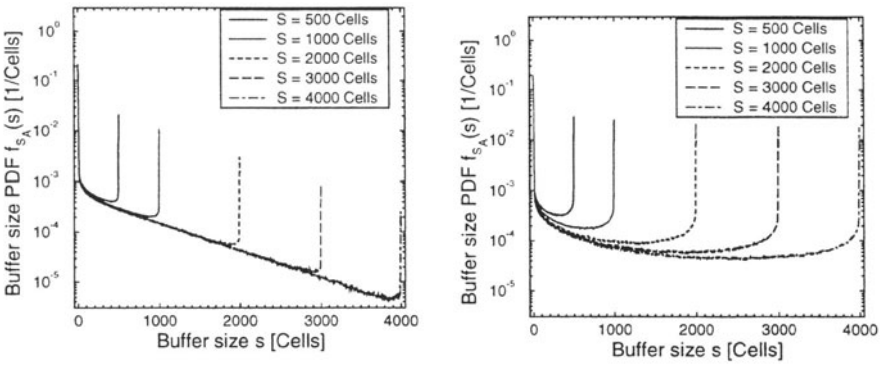

(a) $H = 0.5$ (b) $H = 0.95$

Figure 11 Multiplexer buffer size PDF $f_{S_A}(s)$ depending on the maximum multiplexer buffer size S for pictures with identical PDFs ($A = 0.93$, $N_{\mathbf{Mux}} = 40$)

picture types are used whereas in Figure 9 (b) a single lognormal PDF is used with the parameters of all pictures from Table 1. At large buffer sizes the impact of the Hurst parameter is clearly visible. Video data streams with a high Hurst parameter will cause a cell loss ratio that is orders of magnitude higher than that of streams with a Hurst parameter close to 0.5. Figure 9 also shows that the use of I, P and B pictures gives an additional drop in the cell loss ratio and the slope of its decay is steeper compared to case (b).

The corresponding buffer size PDFs $f_{S_A}(s)$ are depicted in the Figures 10 and 11 for $H = 0.5$ and $H = 0.95$. They have basically the same pot-like

shape, but the decay of the probabilities towards larger buffer sizes heavily depends on the Hurst parameter and the picture types used.

6 CONCLUSIONS

Generally, there are the two alternatives, analysis and simulation, to determine the statistical behaviour of a technical system. Analytical techniques are difficult to apply to complex systems or source models. Thus, many performance evaluation studies are conducted using discrete event simulation. In this paper we studied the impact of complex stochastic processes, that are necessary to realistically characterize VBR MPEG video data streams, on the behaviour of an ATM multiplexer and its evaluation via discrete event simulation. A hierarchical VBR MPEG source model was used to capture the behaviour of such sources at the scene, picture and cell level.

The LRD correlation structures of the stochastic processes used to model the scene level of the video data streams have a significant influence on the simulation duration. In the case of second order self-similar random processes the convergence rate of the mean is directly related to the Hurst parameter. The higher the Hurst parameter H of a stochastic process is, the slower is the decay of the confidence interval size of its mean. For the approximately self-similar ffGn random process, the convergence rate additionally depends on the time span for that the approximation is intended, i. e. the parameter n_{ffGn}.

The multiplexer behaviour in terms of the QoS perceived by the video data streams mirrors the three levels of the video source model. The cell loss rate decreases at three distinct slopes with increasing buffer size according to the fluctuation of the interarrival time introduced by the packetization process, the picture size variation and the long term scene level activity fluctuations. With small buffers, the cell loss rate increases drastically when the ATM segmentation process clusters the cells of individual pictures in bursts instead of smoothing their transfer as good as possible over the picture duration. At medium buffer sizes, the phase relation of the multiplexed VBR MPEG video data streams is essential, since the picture sizes vary periodically in the manner of the GOP structure. If it is possible to influence the mutual phase relations (e. g. by a video server), the cell loss rate can be lowered by several orders of magnitude. Finally, when using large buffers, the degree of long range dependence present in the VBR MPEG video data streams determines the cell loss rate. In any cases the cell delay PDFs have a pot-like shape and their asymmetry is depending on the choice of the source model parameters and the multiplexer buffer size.

REFERENCES

[Cox 84] D. R. Cox, *Long-Range Dependence: A Review*, Statistics: An Appraisal, Proceedings 50th Anniversary Conference Iowa State Statistical Laboratory, H. A. David and H. T. David (Editors), The Iowa State University Press, 1984, pp. 55–74.

[Enss 94] J. Enssle, *Modelling and Statistical Multiplexing of VBR MPEG Compressed Video in ATM Networks*, Proceedings of the 4th Open Workshop on High Speed Networks, Brest, France, September 7–9, 1994, pp. 59–67.

[Enss 95] J. Enssle, *Modelling of Short and Long Term Properties of VBR MPEG Compressed Video in ATM Networks*, Proceedings of the 1995 Silicon Valley Networking Conference & Exposition, San Jose, CA, April 5-7, 1995, pp. 95-107.

[GaWi 94] M. W. Garrett, W. Willinger, *Analysis, Modeling and Generation of Self-Similar VBR Video Traffic*, Computer Communication Review, Vol. 24, No. 4, October 1994, pp. 269–280.

[GFA 96] M. Grasse, M. R. Frater, J. F. Arnold, *Implications of Non-Stationarity in MPEG 2 Video Traffic*, Proceedings of the Seventh International Workshop on Packet Video, Brisbane, March 18–19, 1996.

[HTL 94] D. P. Heyman, A. Tabatabai, T. V. Lakshman, *Statistical Analysis of MPEG-2-Coded VBR Video Traffic*, Proceedings of the Sixth International Workshop on Packet Video, Portland, Oregon, September 26–27, 1994, paper B2.

[Hurs 51] H. E. Hurst, *Long-Term Storage Capacity of Reservoirs*, Trans. Amer. Soc. Civil Eng., Vol. 116, pp. 770–799, 1951.

[KSH 95] M. Krunz, R. Sass, H. Hughes, *Statistical Characteristics and Multiplexing of MPEG Streams*, Proceedings of IEEE INFOCOM '95, Boston, April 4–6, 1995, pp. 455-462.

[Mand 71] B. B. Mandelbrot, *A Fast Fractional Gaussian Noise Generator*, Water Resources Research, Vol. 7, No. 3, 1971, pp. 543–553.

[MaWa 69a] B. B. Mandelbrot, J. R. Wallis, *Computer Experiments with Fractional Gaussian Noises. Parts 1–3*, Water Resources Research, Vol. 5, No. 1, 1969, pp. 228–267.

[MaWa 69b] B. B. Mandelbrot, J. R. Wallis, *Robustness of the Rescaled Range R/S in the Measurement of Noncyclic Long Run Statistical Dependence*, Water Resources Research, Vol. 5, No. 5, 1969, pp. 967–988.

[MPEG 1] ISO/IEC International Standard 11172 (Part 1: System, Part 2: Video, Part 3: Audio), *Information technology — Coding of moving pictures and associated audio for digital storage media up to about 1,5 Mbit/s*, 1993.

[MPEG 2] ISO/IEC Draft International Standard 13818 (Part 1: System (ITU-T Recommendation H.222.0), Part 2: Video (ITU-T Recommendation H.262), Part 3: Audio), *Information technology — Generic coding of moving Pictures and associated audio information*, 1994.

[Rose 95] O. Rose, *Statistical properties of MPEG video traffic and their impact on traffic modeling in ATM systems*, Proceedings of the 20th Conference on Local Computer Networks, Minneapolis, MN, October 16–19, 1995.

[Schu 95] H. Schultze, *Untersuchung des Multiplexverhaltens fraktaler Quellen*, 2. Semesterarbeit, Institut für Nachrichtenvermittlung und Datenverarbeitung, Universität Stuttgart, 1995.